ELSEVIER

Journal of Photochemistry and Photobiology A: Chemistry 130 (2000) 101–111

Journal of Photochemistry and Photobiology A:Chemistry

www.elsevier.nl/locate/jphotochem

Excited-state intramolecular proton transfer (ESIPT) in 2-(2′-hydroxyphenyl)-oxazole and -thiazole

Denis LeGourriérec [a,*], Vladimir A. Kharlanov[b,1], Robert G. Brown [a], Wolfgang Rettig [b]

[a] *Centre for Photochemistry, Maudland Building, University of Central Lancashire, Preston, Lancashire PR1 2HE, England, UK*

[b] *Institut für Physikalische und Theorische Chemie, Humboldt-Universität Berlin, Bunsenstraße 1, D-10117 Berlin, Germany*

Received 24 May 1999; accepted 3 October 1999

Abstract

The azoles 2-(2′-hydroxyphenyl)oxazole (HPO) and 2-(2′-hydroxyphenyl)-4-methylthiazole (HPT) have been synthesised and studied in order to compare their photophysical characteristics. Their absorption and emission properties are reported in non-polar, alcoholic and aqueous media. Ground and excited state p*K* data were determined by spectroscopy and a model is proposed to explain the behaviour of HPT and HPO as a function of the pH. Excitation spectra and quantum chemical calculations suggest an equilibrium of ground state conformers. The calculations also predict a small energy barrier for rotation in the first excited singlet state for the proton transferred tautomers. The resulting twisted structure of the tautomer form possesses a biradicaloid nature, and is near-degenerate in energy with the first excited triplet state.

Keywords: Fluorescence; Proton transfer; Ab initio calculations

1. Introduction

Amongst the large range of systems undergoing excited-state intramolecular proton transfer (ESIPT) [1–3], compounds of the azole type form an important class of their own. The earliest studies by Passerini [4,5] and Cohen and Flavian [6] on 2-(2′-hydroxyphenyl)benzoxazole (HPBO) and 2-(2′-hydroxyphenyl)benzothiazole (HPBT) have since been much extended [7–12]. Comparative studies have been reported, including also the related 2-(2′-hydroxyphenyl)benzimidazole HPBI [13–16] and 2-(2′-hydroxy-5′-methylphenyl)benzotriazole (trade name Tinuvin-P/TIN-P) [16–18].

The azoles HPBO, HPBT and HBPI exhibit dual emission in polar solvents. It has been shown that different species coexist in the ground state [8,12,15,17] and only the closed enol conformer (denoted OHc-*cis*, see Scheme 1 for molecules studied in this work) gives the Stokes shifted emission after undergoing ESIPT. Other conformers are responsible for the normal emission: an open *cis*-enol species (OHo-*cis* which is hydrogen-bonded to a solvent molecule) and *trans*-conformers, with a hydrogen bond involving the second heteroatom (O or S, see structure OHc-*trans*, Scheme 1) or the solvent (OHo-*trans*).

The differences in the photophysical properties of HPBO and HPBT have been rationalised by several authors [19,20]. For HPBT, both *cis* and *trans* isomeric proton transfer (PT) tautomers exist in the excited state, but there is only a *cis* conformer in the case of HPBO. These authors proposed that the linkage joining the benzazole moiety and the phenol ring has more single-bond character in the PT tautomer of HPBT, facilitating the formation of rotamers of type NH-90 (see Scheme 2). The origin of this difference lies in the lower electronegativity of the sulfur, compared with that of

* Corresponding author. Present address: School of Chemical Sciences, Dublin City University, Glasnevin, Dublin 9, Ireland. Fax: +353-01-704-5503.

E-mail addresses: denis.legourrierec@dcu.ie (D. LeGourriérec), vlad@ipoc.rnd.runnet.ru (V.A. Kharlanov).

[1] Present address: Research Institute of Physical and Organic Chemistry, Rostov State University, pr. Stachki 194/3, Rostov-on-Don, 344104 Russia.

Abbreviations: BESSY, Berliner Elektronenspeicherring-Gesellschaft für Synchrotronstrahlung mbH; ESIPT, excited-state intramolecular proton transfer; HPBI, 2-(2′-hydroxyphenyl)benzimidazole; HPBO, 2-(2′-hydroxyphenyl)benzoxazole; HPO, 2-(2′-hydroxyphenyl)oxazole; HPBT, 2-(2′-hydroxyphenyl)benzothiazole; HPT, 2-(2′-hydroxyphenyl)-4-methylthiazole; IMHB, intramolecular hydrogen bond; MCH, methylcyclohexane; PT, proton transfer; TIN-P, trade name Tinuvin-P: 2-(2′-hydroxy-5′-methylphenyl)benzotriazole

1010-6030/00/$ – see front matter
PII: S1010-6030(99)00206-3

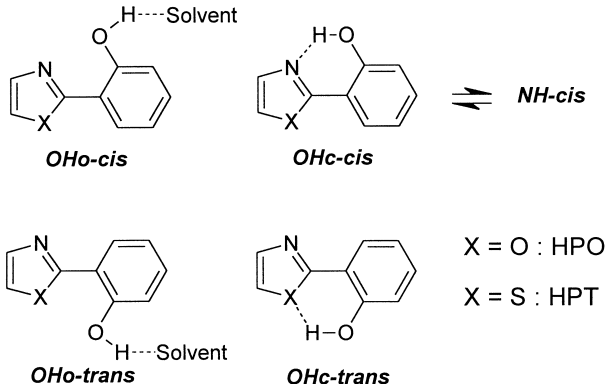

Scheme 1. Possible OH-forms of HPO and HPT (the 4-methyl substituent for HPT is not shown).

oxygen. For the azole system in HPBT, this means a better delocalisation of the p electrons, a higher nitrogen basicity [21,22], and less chance of hydrogen bonding involving the second heteroatom as in rotamer OHc-*trans* [2].

The majority of the studies to this date have concentrated on the benzazoles rather than the analogues without the fused benzo ring. Two papers by Douhal and co-workers deal with phenyl substituted derivatives of 2-(2′-hydroxyphenyl)oxazole (HPO). In a first publication [23], the 0-0 transition was reported at 29852 cm^{-1} under supersonic jet conditions, followed by a very fast (>4.5×10^{12} s^{-1}) ESIPT reaction. The second paper [24] deals with rotational processes. On the basis of experimental and theoretical results, it is concluded that two rotamers of type OHc-*cis* and OHc-*trans* (see Scheme 1) coexist in the ground state, the former being more stable and the only one able to undergo ESIPT. In the excited state, the ESIPT reaction has a small or zero energy barrier and the keto tautomer once formed can undergo 180° twist. To our knowledge, no work has been reported on 2-(2′-hydroxyphenyl)-4-methylthiazole (HPT).

In this paper, we present the results of a comparative study involving the azoles HPO and HPT (Scheme 1). Their emission and absorption properties are reported in non-polar, polar, alcoholic and aqueous environments. The photophysical characteristics are discussed according to the nature of the heteroatom and involving a rotational mechanisms. Quantum chemical calculations are used to help predict possible conformers.

2. Materials and methods

2.1. Materials

2.1.1. 2-(2′-Hydroxyphenyl)oxazole (HPO)

The Pomeranz–Fritsch synthesis of isoquinolines involves the intramolecular cyclisation of (2-nitrobenzalamino) acetaldehyde diethyl acetal [25]. The yield is generally high with electron releasing groups (e.g. methoxy or methyl substituents) but no isoquinoline is obtained with electron withdrawing groups (e.g. nitro substituents). In this case, the products are oxazoles. This method was used to prepare 2-(2′-nitrophenyl)oxazole from 2-nitro-benzaldehyde [26]. Reduction of 2-(2′-nitrophenyl)oxazole was achieved with 10% palladium on carbon (Pd/C) in methanol according to the procedure of Bavin [27] affording 2-(2′-aminophenyl)oxazole which was then diazotized [28]. Decomposition of the diazonium salt afforded HPO.

2.1.2. 2-(2′-Aminophenyl)oxazole [27]

A solution of 2-(2′-nitrophenyl)oxazole [26] (2 g, 0.01 mol) in 95% ethanol (15 ml) was warmed to 50°C, whereupon 10% Pd/C (15 mg, previously moistened with alcohol) was added. Hydrazine hydrate (ca. 1.3 ml) was added to the stirred mixture over 10 min. At this point, an additional amount of Pd/C (15 mg) was added and the mixture was refluxed for 1 h. The catalyst was removed by filtration through a thin layer of Celite™ and the solution was concentrated at reduced pressure to give 2-(2′-aminophenyl)oxazole (1.25 g; 74%) as an oil which solidified on cooling to give colourless crystals, m.p. 31–32°C (lit. 32–33°C [25]). It was easily recognisable on TLC by its

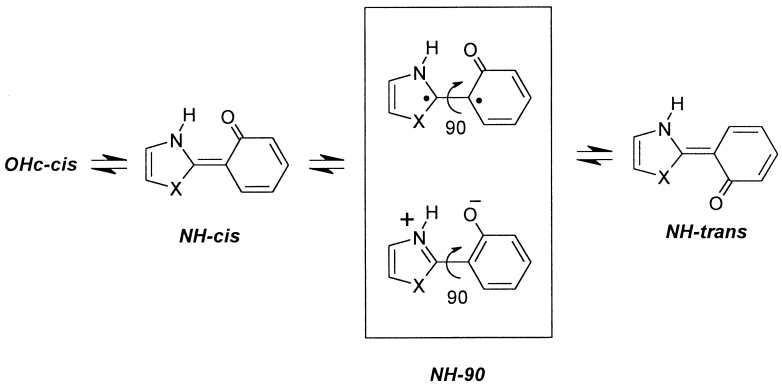

Scheme 2. Possible NH-forms of HPO and HPT (the 4-methyl substituent for HPT is not shown).

blue fluorescence. It was used within a few days but can be kept in a refrigerator, under nitrogen for long term storage.

MS: *m/z* 160 (M^+), 131, 104, 90, 77

2.1.3. 2-(2′-Hydroxyphenyl)oxazole (HPO)

2-(2′-Aminophenyl)oxazole (0.64 g, 4 mmol) was dissolved in hot concentrated sulfuric acid (4 ml) and then cooled below 15°C. Ice (ca. 4 g) was added when the amine bisulfate separated. A solution of sodium nitrite (0.35 g, 5.07 mmol) in ice water (4 ml) was added dropwise under the surface of the ice cooled, stirred amine solution, at such a rate that the temperature remained below 5°C. After the addition was complete, the mixture was stirred for an additional 5 min and then a few crystals of urea were added to decompose the excess of sodium nitrite. The cold (0°C) solution was treated with a solution of copper(II) nitrate trihydrate (15 g) in water (140 ml) and copper(I) oxide (0.53 g, 55 mmol) was added to the vigorously stirred solution. The mixture was extracted with diethyl ether, the extracts were dried (Na_2SO_4) and evaporated and the residue was purified by flash chromatography (10% ethyl acetate/light petroleum b.p. 60–80°C). The resulting oil crystallised on cooling and was recrystallised from aqueous ethanol to afford 2-(2′-hydroxyphenyl)oxazole (50 mg; 10%), m.p. 36–37°C, as colourless needles.

NMR: δ_H 6.94 (1H, m, 5′-H), 7.10 (1H, dd, 3′-H), 7.27 (1H, d, 4-H), 7.40 (1H, m, 4′-H), 7.75 (1H, d, 5-H), 7.86 (1H, dd, 6′-H), 11.2 (1H, s, OH)

MS: *m/z* 161 (M+), 132, 105, 78

2.1.4. 2-(2′-Hydroxyphenyl)-4-methylthiazole (HPT)

Müslin et al. [29] synthesised 2-(2′-hydroxyphenyl)thiazole from 2-hydroxythiobenzamide and bromoacetaldehyde. Bromoacetone was preferred in the current work since it is more readily available. The same procedure was followed, thus giving a methyl substituted product. We assume that the presence of the 4-methyl substituent in HPT has no major effects on the spectroscopy and dynamics of HPT (as Guallar et al. proposed in the case of HPO [24]),

A solution of 2-hydroxythiobenzamide [30] (0.4 g, 2.61 mmol), bromoacetone [31] (0.56 g, 2.61 mmol) in ethanol (1 ml) and piperidine (0.1 ml) was refluxed for 7 h. The alcohol was evaporated and the residue was extracted with diethyl ether (3×50 ml) and the extracts were washed with aqueous potassium carbonate (50 ml). The ether extracts were dried ($MgSO_4$) and treated with a vigorous stream of dry hydrogen chloride gas (generated by dropping concentrated sulfuric acid onto ammonium chloride previously wetted with concentrated hydrochloric acid [28]). The resulting brown crystals were filtered off and added to a potassium hydrogen carbonate solution as to basify the mixture. Extraction with diethyl ether (15 ml) and removal of the dried (Na_2SO_4) solvent gave a brown residue which was distilled under reduced pressure to afford HPT as an oil (b.p. 100°C at 13 mm Hg) that crystallised on standing. Subsequent recrystallisation from aqueous methanol gave the pure material (0.2 g; 40%), m.p. 62–63°C.

NMR: δ_H 2.50 (3H, s, OCH_3), 6.83 (1H, s, 5-H), 6.93 (1H, m, 5′-H), 7.06 (1H, dd, 3′-H), 7.29 (1H, m, 4′-H), 7.62 (1H, dd, 6′-H), 12.4 (1H, s, OH)

MS: m/z 191 (M^+), 163, 146, 118, 71

2.1.5. 2-(2′-Hydroxyphenyl)benzothiazole (HPBT) and 2-(2′-hydroxyphenyl)benzoxazole (HPBO)

HPBT was prepared by C.A.S. Potter according to the published method [32] and was recrystallised from 1-butanol. HPBO was synthesised by K.W. Hodgson [33] and was recrystallised from aqueous ethanol.

2.2. Methods

Absorption spectra were recorded on a Hewlett–Packard HP8452A diode array spectrophotometer using 1 cm path-length quartz cells. Corrected fluorescence spectra (in spectroscopic grade solvents, Merck or Aldrich) were recorded on a SPEX Fluoromax spectrofluorimeter and fluorescence quantum yields were determined relative to quinine sulfate in 0.1 M perchloric acid ($\Phi_f = 0.55$) [34]. Room temperature fluorescence lifetime measurements were undertaken at the Daresbury Synchrotron Radiation Source (in single bunch mode) as described elsewhere [35] and on a laser system at Imperial College, London. In the latter case, the excitation light (300 nm, 50 ps pulse length) was obtained by frequency doubling the 600 nm output of a dye laser (rhodamine 6G). Variable temperature fluorescence decay measurements were carried out using synchrotron radiation from BESSY (in single bunch mode) as the source of excitation. The equipment has been described previously [36]. In all cases, the time-correlated, single photon counting method [37] was used to accumulate fluorescence lifetime data. An iterative reconvolution program was used to analyse the decays and the χ^2 value together with the distribution of the residuals were examined to estimate the quality of the fit. Lifetimes down to approximately 0.1 ns could be obtained using the BESSY and Daresbury synchrotrons and the laser system allowed us to analyse the decays down to approximately 10 ps. ^{1}H NMR spectra were recorded in deuterated chloroform on a Brucker W250 instrument. Ionisation constants (p*K*) were determined spectroscopically [38] (estimated $\pm$ 0.1) and the excited state pK^* values were calculated by the Förster cycle method and by fluorescence titration.

3. Results and discussion

3.1. Absorption spectra

The absorption spectra of HPO and HPT and of HPBO and HPBT in methylcyclohexane are compared in Fig. 1. The spectra are normalised to the same absorbance for the long

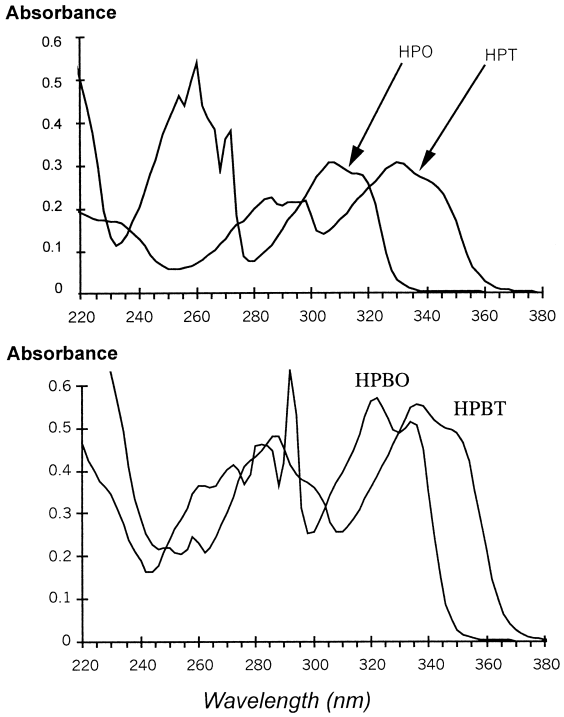

Fig. 1. Absorption spectra of HPO, HPT, HPBO and HPBT in MCH (2.5×10^{-5} M, normalised).

wavelength band. The long wavelength band (>300 nm) has been attributed to a π-π^* state with charge transfer character [39] whilst the band in the region 240–290 nm is due to the azole chromophore [24,39]. The extinction coefficients in ethanol ($\varepsilon = 6300$–$7600\,\mathrm{dm^3\,mol^{-1}\,cm^{-1}}$) are of the same order for HPO and HPT (see Table 1). The absorption data for HPO compares well with those of the phenyl substituted derivative studied by Guallar et al. [24].

Substitution of oxygen for sulfur causes a red shift of approximately 20 nm, probably due to better delocalisation of the electrons in the thiazoles than in the oxazole, which has less aromatic character [21,22]. The absorption spectra of the thiazoles are more diffused than those of the oxazoles. This is especially obvious for the 250–300 nm band. The interpretation proposed in previous work on HPBT and HPBO [19,20] also holds for HPT and HPO, i.e. the linkage between the phenol and the azole rings has more single bond character in the thiazoles allowing for more twisting vibrations and formation of rotamers (e.g. OHc-*trans*) and hence a more diffuse absorption spectrum.

The benzo analogues HPBT and HPBO possess higher extinction coefficients ($\varepsilon = 12\,000$–$14\,000\,\mathrm{dm^3\,mol^{-1}\,cm^{-1}}$ [8,9], compared to ca. $7000\,\mathrm{dm^3\,mol^{-1}\,cm^{-1}}$ for HPO and HPT) and their absorption spectra are red-shifted (10–20 nm) compared to HPO and HPT, as expected due to the extension of the conjugated system.

3.2. Fluorescence measurements

Fluorescence from the PT tautomer in non-polar solvents was observed with similar Stokes shifts for both compounds (see Table 1 for photophysical properties in MCH). A very weak blue fluorescence band was also observed for HPO (340 nm, see Fig. 2), which Guallar et al. [24] also mention for the methyl substituted derivative of HPO. These authors assigned this band to the *trans* enol species (tautomer OHc-*trans* in Scheme 1). The PT fluorescence from HPO appears at shorter wavelengths compared to HPT and also has a slightly higher quantum yield. In polar and protic solvent (see Table 1), normal and Stokes shifted fluorescence bands were observed from HPO and HPT, and were attributed to the enol and PT species, respectively. The emission spectra

Table 1
Photophysical properties of HPO and HPT in various solvents at room temperature[a]

Sample	Solvent	Absorption	Emission						
		λ_{max} (nm)	Band	λ_{max} (nm)	Φ_f	Lifetime			Stokes shift (cm^{-1})
						τ (ns)	Amplitude	$\langle\tau\rangle$ (ns)	
HPO	Ethanol	306	Enol	345	0.0035	1.55	0.86	1.37	3700
		(316)				0.28	0.14		
		$\varepsilon = 7600$	PT	460	0.0131	0.43	1	0.43	11000
	Acetonitrile	306	Enol	345	<0.002	–	–	–	3700
		(314)	PT	465	0.0060	0.19	1	0.19	11200
	MCH	310–320	Enol	340	<0.001	–	–	–	1800
			PT	480	0.0072	0.21	1	0.21	10400
HPT	Ethanol	326	Enol	360	0.010	0.69	0.83	0.58	2900
		(334)				0.021		0.17	
		$\varepsilon = 6300$	PT	505	0.0087	0.16	0.67	0.25	10900
						0.44	0.33		
			Enol	350	<0.002	–	–	–	2100
	Acetonitrile	326	PT	513	0.0019	0.59	<0.01	0.08	11200
		(334)				0.08	>0.99		
	MCH	330 (340)	PT	525	0.0032	0.86	1	0.86	10400

[a] ε in $\mathrm{dm^3\,mol^{-1}\,cm^{-1}}$

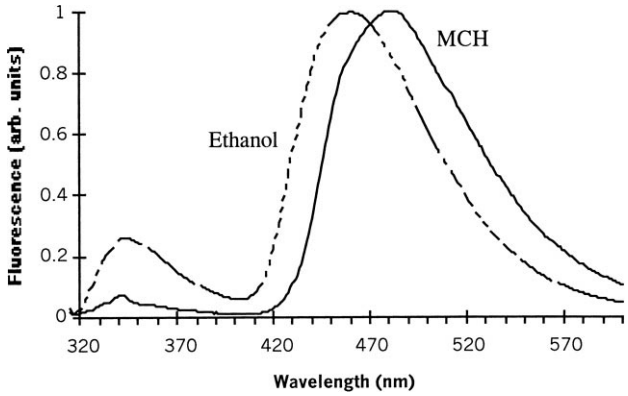

Fig. 2. Normalised emission spectra of HPO in ethanol and MCH (ca. 2.5×10^{-5} M).

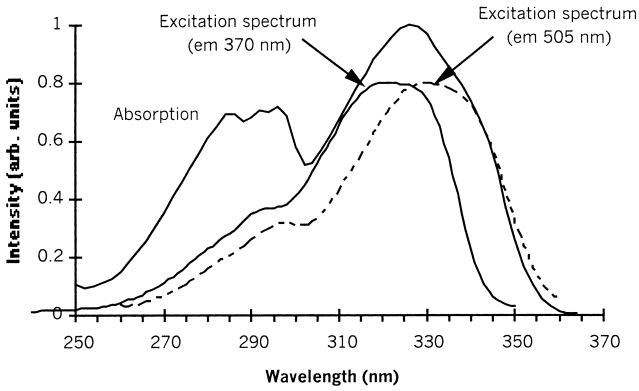

Fig. 5. Excitation and absorption spectra of HPT in ethanol (ca. 7.9×10^{-6}M, normalised).

are shown in Figs. 2 and 3 in ethanol and MCH. For both compounds, a blue shift of the PT band was observed in the polar protic solvents compared to MCH. This observation is similar to 3-hydroxy-2,2′-bipyridyl, interpreted there, based on low temperature lifetimes, as indicating specific hydrogen bonding of the PT species [40]. For both compounds in protic solvent, the intensity ratio of the normal and PT bands varied with excitation wavelength. The excitation spectra (see Figs. 4 and 5) of the enol and PT bands were found

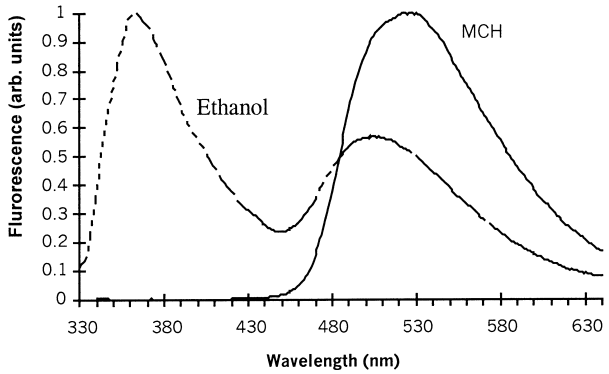

Fig. 3. Normalised emission spectra of HPT in ethanol and MCH (ca. 5.0×10^{-5} M).

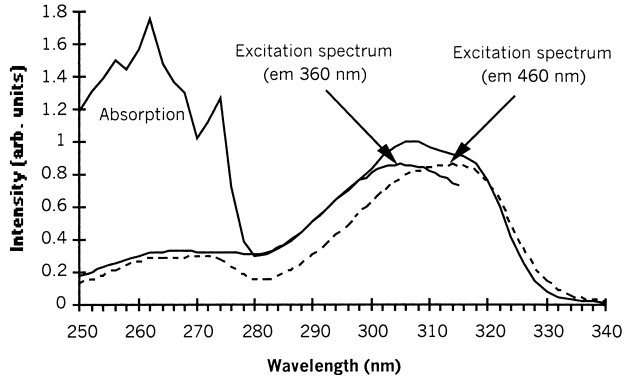

Fig. 4. Excitation and absorption spectra of HPO in ethanol (ca. 6.5×10^{-5} M, normalised).

to be different and did not match the absorption spectrum. It is also worth noting that the excitation spectra of the keto bands in acetonitrile were very similar to those in MCH.

These observations suggest the existence of two ground state species in equilibrium which possess different absorption properties. One species is responsible for the proton transfer fluorescence exclusively while the other causes the normal emission band, as explained earlier. The same observations were made for HPO [24] and HPBO [15,41]. For HPBT, however, the excitation spectrum for the enol and PT fluorescence are identical [7], and give no evidence for distinct ground state species.

The excitation wavelength dependence of the emission means that the quantum yields of enol and PT emission for HPO and HPT (see in Table 1) are only valid for the given excitation wavelength. For both the plain azoles and their benzologues [15,35], the enol emission is more intense than the PT emission in the thiazoles, whereas the opposite is true for the oxazoles. A higher quantum yield for PT than for normal fluorescence suggests that either the equilibrium in the ground state is displaced towards the species responsible for PT emission or that some excited state mechanism that depopulates the emitting state is absent. One must bear in mind that the amount of exciting radiation absorbed by the species responsible for the enol and PT emission bands is not known.

Mono- or bi-exponential fluorescence decays were measured in polar and non-polar solvents (Table 1). The lifetimes and quantum yields in acetonitrile for the enol band could not be determined accurately because of the non-negligible residual fluorescence from the solvent under the wavelength conditions used, combined with a weak emission. Shorter lifetimes and lower quantum yields were found for the PT band in acetonitrile, compared to ethanol and MCH. A variable temperature study in MCH showed that the lifetimes increased from 0.21 to 6.7 ns for HPO and from 0.86 to 5.42 ns for HPT when the temperature is lowered from 298 down to 133 K. A similar, strong temperature dependence was observed for the benzo analogues HPBO [7] and HPBT

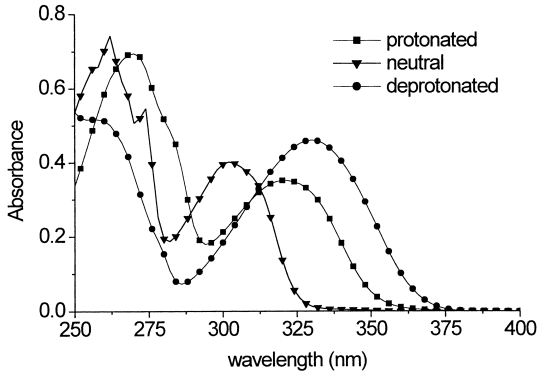

Fig. 6. Absorption spectra of HPO in water at pH = 1.00 (■), pH = 8.00 (▼) and pH = 11.30 (●) (ca. 5×10^{-5} M).

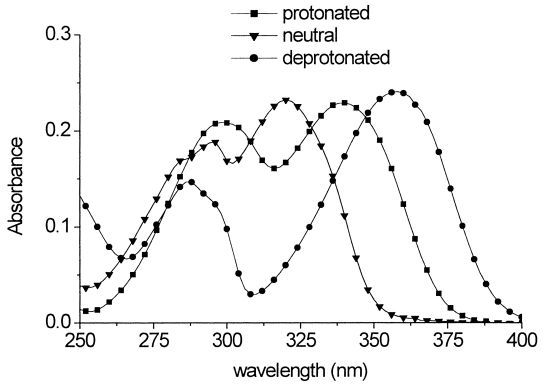

Fig. 7. Absorption spectra of HPT in water at pH = 2.00 (■), pH = 7.40 (▼) and pH = 10.90 (●) (ca. 5.0×10^{-5} M).

[42]. The corresponding fluorescence spectra as a function of temperature for HPO and HPT were not measured.

3.3. Effects of the pH on the absorption and fluorescence properties

3.3.1. Absorption properties in aqueous solution

HPO and HPT are readily protonated and deprotonated and the absorption spectra of their different forms as a function of pH are shown in Figs. 6 and 7. Ionisation constants were calculated from the spectral data according to [38] and are given in Table 2, along with the absorption maxima (λ_{max}) and the isobestic points (λ_{iso}). The pK_2* values for deprotonation were calculated (Förster cycle) using the average of the absorption and emission maxima (in wavenumbers). The pK_1* values for protonation were calculated from the absorption wavelengths only because the protonated species is non-fluorescent, as explained later.

Table 2 shows that the pK_1 value of the thiazole HPT (2.7) is higher than that of the oxazole HPO (2.01) and the same is true for their benzo counterparts HPBT (1.16 [7]) and HPBO (−0.3 [10]). This is in agreement with the weaker basicity of the oxazoles compared to the thiazoles [21,22]. The pK_2 values are slightly lower for HPT (8.8) than for HPO (9.5), and for HPBT (10.3 [7], 10.16 [4,5]) as compared to HPBO (10.4 [10], 10.48 [14]). Roberts et al. [14] propose that HPBT is less planar than HPBO, and possesses a weaker intramolecular hydrogen bond (IMHB), hence a pK_2 which is closer to that of non-hydrogen bonded phenols.

3.3.2. Fluorescence properties

The changes in the fluorescence spectra of HPO and HPT when exciting at the isosbestic points given in Table 2 are shown in Figs. 8–11. A similar behavior was observed for both compounds. The ionisation constants have also been determined from the fluorescence data (see Table 2). These pK values are similar to those calculated by absorptiometric titration and reflect the fact that the emission spectra are largely determined by the nature of the absorbing species.

At low pH, weak emission is observed (band A: near 445 nm for HPO and 500 nm for HPT). As the pH is raised to neutral, the fluorescence peak blue-shifts (to band B: 410 nm for HPO and 445 nm for HPT) and the emission increases in intensity. A shoulder also appears (band C: around 350 nm for HPO and 370 nm for HPT). As the pH is further increased, the shoulders disappear, and the remaining emission band B becomes stronger and is the only one present at high pH.

At neutral pH, the uncharged enol HPO or HPT molecules are expected to be the dominant species in solution (on the basis of the pK values) but the fluorescence spectra (see Figs. 9 and 11) appear to consist of more than one band. Fluorescence decay profiles in neutral aqueous solution were

Table 2
Photophysical properties of HPO and HPT in aqueous solution

		Absorption				Fluorescence			
		S_0 pK	S_1 pK*	λ_{iso} (nm)	λ_{max} (nm)	pK	λ_{max} (nm)	Φ_f	τ (ns)
HPO	HPO^-H^+ (pK_1)	2.01	7.86	315	320	2.50	–	–	–
	Neutral species				302		E: 350 (C)	0.012	0.16
							PT: 445 (A)	0.003	0.06
	HPO^- (pK_2)	9.0–9.5	1.7–2.2	315	330	9.26	410 (B)	0.18	2.45
HPT	HPT-H^+ (pK_1)	2.7	6.6	328	340	2.98	–	–	–
	Neutral species				320		E: 370 (C)	0.035	0.12
							PT: 500 (A)	0.008	0.03
	HPT^- (pK_2)	8.8	0.54	335	358	9.4	445 (B)	0.20	2.0

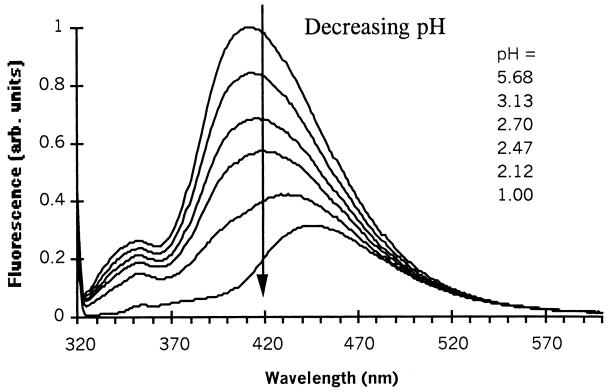

Fig. 8. Emission spectra of HPO in water with decreasing pH (ca. 5.0×10^{-5} M). Band A (445 nm): proton transferred species, Band B (410 nm): HPO^{-}, Band C (350 nm): neutral enol form.

measured at different wavelengths across the emission band and the analysis is reported in Table 3. At least three different emitting species, with distinct lifetimes can be distinguished from these data, suggesting the existence of prototropic ground state equilibria.

According to these observations, we propose the following interpretation. Band C may be assigned to the neutral

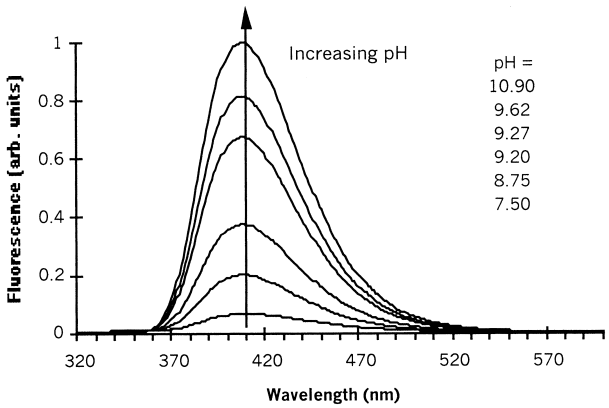

Fig. 9. Emission spectra of HPO in water with increasing pH (ca. 5.0×10^{-5} M). Band B (445 nm): HPO^{-}.

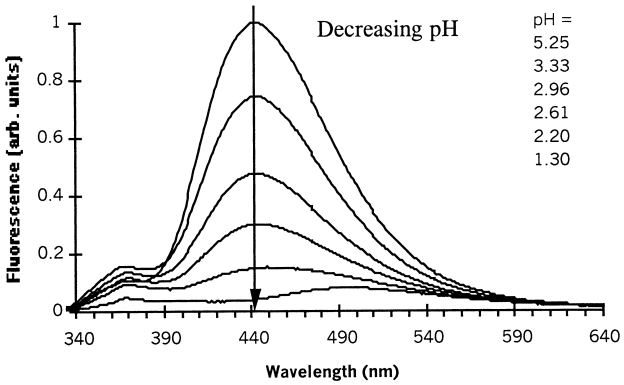

Fig. 10. Emission spectra of HPT in water with decreasing pH (ca. 5.0×10^{-5} M). Band A (500 nm): proton transferred species, Band B (445 nm): HPT^{-}, Band C (370 nm): neutral enol form.

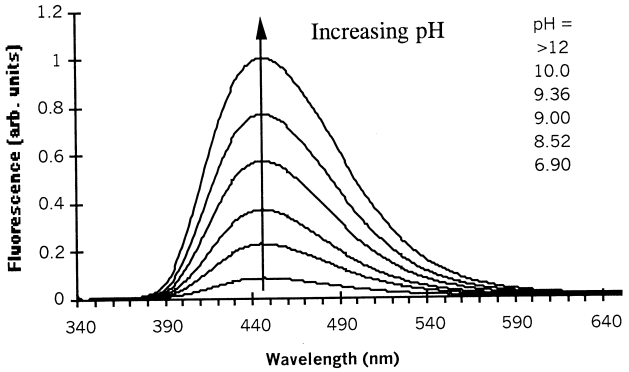

Fig. 11. Emission spectra of HPT in water with increasing pH (ca. 5.0×10^{-5} M). Band B (445 nm): HPT^{-}.

enol species on the basis of the wavelength, although the main lifetime components are much shorter than those measured in ethanol (see Table 2). The main lifetime component of the band B is close to the value found in basic conditions (2.45 and 2.00 ns for HPO and HPT, respectively). The position of this band is also similar under neutral and basic conditions. We therefore assign this band to the deprotonated species (HPX-). The weak band A observed under acidic conditions is too strongly Stokes shifted (10 600 cm^{-1}) to correspond to the protonated form HPX-H^{+*}. On the basis of the emission wavelength we propose that this band is due to the PT tautomer (λ_{em} in ethanol 460 nm). The very short lifetimes measured for this band were also present at neutral pH, on the red edge of the spectrum and at 410 nm for the deprotonated species, in basic conditions. According to this model, we conclude that the protonated form (HPX-H^{+*}) does not fluoresce.

The mechanism in Scheme 3 is proposed to summarise the possible behaviour of HPO and HPT in aqueous solu-

Table 3
Analysis of fluorescence decay profiles for HPO and HPT in water at neutral pH

Sample	λ_{em} (nm)	τ (ns)	Amplitude	%	
HPO	350	0.0591	0.28	11.4	1.11
		1.51	0.01	10.4	
		0.16	0.71	78.2	
	410	0.060	0.58	4.1	1.29
		2.36	0.33	92.7	
		0.29	0.09	3.1	
	480	0.060	0.96	44.1	1.22
		2.32	0.03	53.3	
		0.34	0.01	2.6	
HPT	370	0.028	0.52	16.0	1.25
		2.04	0.01	22.3	
		0.12	0.47	61.7	
	445	1.95	0.12	67.1	1.08
		0.094	0.51	13.8	
		0.18	0.37	19.1	
	500	0.031	0.31	3.5	1.06
		1.88	0.07	47.4	
		0.22	0.62	49.1	

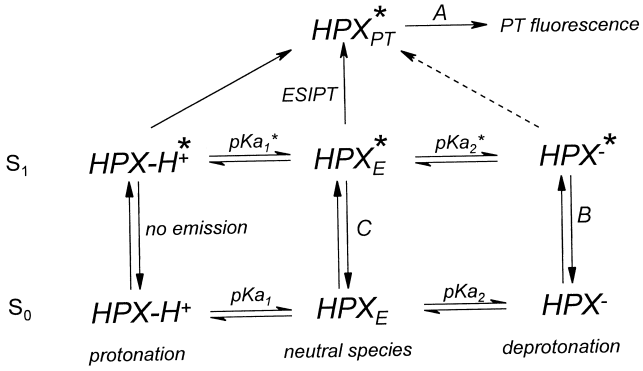

Scheme 3. Model for the photophysics of HPO and HPT in aqueous solution.

tion. Although not all arrows indicated have been evidenced by the present work, this scheme is intended to give an overall view. At pH ≈ 1, the PT tautomer may be obtained by deprotonation of the hydroxyl group of the *cis*-isomer of HPX-H^{+*}. Although this should only occur at pH > pK_2^*, it is possible that the protonated nitrogen atom of HPX-H^{+*} provides a driving force for this mechanism. Whether the PT tautomer is also obtained by protonation of the nitrogen of HPO^- and HPT^- is more uncertain because of the very low concentration of protons under basic conditions. Therefore, the 0.067 ns component found at 410 nm at pH ≈ 10 for HPO may not be related to the 0.06 ns lifetime of the keto tautomer.

The lifetime of the proton transfer HPT tautomer (neutral pH, see Table 3) is not exactly the same throughout this analysis but it appears to be near 0.03 ns. The variation in lifetime is understandable given the time resolution of the instrumentation. The origin of the 0.22 ns component at 500 nm in neutral conditions is unclear.

3.4. Quantum chemical calculations

Calculations of all conformers of HPO and HPT (Schemes 1 and 2) in the ground and excited states were carried out using the GAUSSIAN 94 program [43] with the HF method and a 3-21G* basis set with vibrational analysis of the geometry-optimised structure. Excited-state geometry optimisations were calculated by the interaction of singly excited configurations (CIS) involving 20 occupied and 20 unoccupied orbitals.

3.4.1. OH-type conformers in the ground state

HPO and HPT in the ground state possess different stable OH-type conformers (Table 4, Scheme 1). A thermal equilibrium of these conformers is consistent with the excitation wavelength dependence of the observed fluorescence spectra (see Figs. 4 and 5). The OHc-*cis* conformation of HPO and HPT is determined to be the most stable species. For HPO, our results are in close agreement with previous calculations [24]. It can be noted that the *trans* isomer is more stabilised with respect to the *cis* isomer for HPO than for HPT (see Table 4), indicating the better ability of oxygen to form a hydrogen bond, as compared to sulfur.

Table 4
Relative energy (in kcal/mol) of the stable OH-type conformers of HPO and HPT in the ground state as determined by HF/3–21G* optimisations

	OHo-*trans*	OHo-*cis*	OHc-*trans*	OHc-*cis*
HPO	15.24	14.14	4.23	0
HPT	6.68	15.10	13.5	0

Table 5
Relative energy (in kcal/mol) of the stable NH-type conformers of HPO and HPT in the ground state, as well as the transition state NH-90, as determined by HF/3–21G* optimisations

	NH-*cis*	NH-90	NH-*trans*
HPO	0	37.12	20.70
HPT	0	35.13	7.09

3.4.2. NH-type conformers in the ground state

There exist two stable forms (NH-*cis* and NH-*trans*) in the S_0-state with a transition structure (NH-90) separating the two minima (Table 5 and Fig. 12). The most stable conformer is the NH-*cis* form. NH-90 possesses a zwitterionic electronic structure with a large dipole moment of ca. 9D (Tables 6 and 7).

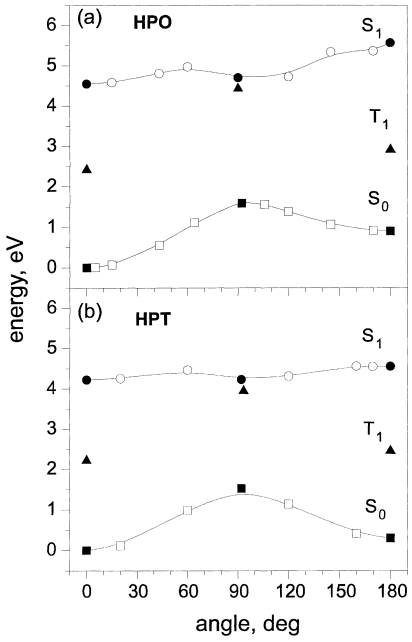

Fig. 12. S_1-, T_1- and S_0-state surfaces as calculated for the internal rotation of the fragments of the NH-type conformers of HPO (a) and HPT (b). The origin of the energy axis corresponds to −545.9697154 a.u. (HPO) and to −867.2014670 a.u. (HPT).; 0 deg correspond to the NH-*cis* and 180 deg to the NH-*trans* conformer. Filled symbols correspond to full optimisation (minima or saddle points), open symbols to optimisation with fixed twist angle.

Table 6
Properties of the energy minima and the transition state of the excited state NH-type conformers of HPO

State characteristic	NH-*cis*	NH-90	NH-*trans*
Point Group	C_s	C_1	C_s
$S_1 \rightarrow S_0$ transition energy, eV	4.23	1.84	4.38
Oscillator strength	0.4431	0.0000	0.0000
$S_1 - T_1$ energy gap, eV	1.92	0.12	2.30
Dipole moment of the S_1 (S_0) State, D[a]	4.59 (5.72)	2.97 (8.76)	4.82 (7.75)
Vectorial dipole moment change of S_1–S_0, D	1.12	8.75	7.81
State assignment	π-π^*	Biradicaloid	(n-π^*)[b]

[a] The dipole moment vectors are not always parallel.
[b] The lowest π-π^* state is 4.72 eV above the S_0 state.

Table 7
Properties of the energy minima and the transition state of the excited state NH-type conformers of HPT

State characteristic	NH-*cis*	NH-90	NH-*trans*
Point group	C_s	C_1	C_s
$S_1 \rightarrow S_0$ transition energy, eV	3.97	2.12	3.97
Oscillator strength	0.5792	0.0002	0.5020
$S_1 - T_1$ energy gap, eV	1.80	0.07	1.91
Dipole moment of the S_1 (S_0) state, in D[a]	3.89 (5.17)	3.77 (8.95)	6.71 (7.30)
Vectorial dipole moment change of S_1–S_0, (in D)	1.28	9.09	0.78
State nature	π-π^*	Biradicaloid	(π-π^*)[b]

[a] The dipole moment vectors are not always parallel.
[b] The lowest n-π^* state is 5.13 eV above the S_0 state.

3.4.3. NH-type conformers in the S_1-state

Fig. 12 summarises the calculations for ground and excited states of the NH-type conformers of HPO and HPT. The rather large barrier in the ground state contrasts with a slight energy minimum of the excited state, for the near perpendicular conformation NH-90. It is remarkable that the optimised NH-90 structure of the ground state corresponds to two virtually planar subsystems twisted orthogonally to each other (compare the dihedral angles in Tables 8 and 9). The optimisation of the S_1 minimum, starting with the NH-90 structure of the ground state, however, leads to significant deviations from this locally planar structure to a bent

Table 8
Selected bond lengths and angles of the NH-type conformers of HPO in the optimised S_0 and S_1-states by HF/3–21G*. For the atom numbering, see Fig. 13

Bond length, dihedral angle (Å, deg)	NH-*cis*		NH-90		NH-*trans*	
	S_0-state	S_1-state	S_0-states	S_1-state	S_0-states	S_1-state
2–1	1.3313	1.3513	1.3181	1.4076	1.3628	1.3883
2–6	1.3835	1.3914	1.4383	1.4464	1.3663	1.3454
6–7	1.4417	1.5015	1.4311	1.4651	1.4636	1.4617
11–6	1.4197	1.3792	1.3953	1.4033	1.4415	1.4535
7–12	1.2615	1.2006	1.2565	1.2314	1.2286	1.2969
α (7, 6, 2, 1)	0	0	90	61.8	180	180
β (6, 2, 1, 5)	180	180	180	138.1	180	180

Table 9
Selected bond lengths and dihedral angles of the NH-type conformers of HPT in the optimised S_0 and S_1-states by HF/3–21G*. For the atom numbering, see Fig. 13

Bond length, angle (Å, deg)	NH-*cis*		NH-90		NH-*trans*	
	S_0-state	S_1-state	S_0-state	S_1-state	S_0-state	S_1-state
2–1	1.3354	1.3625	1.3189	1.4096	1.3507	1.3721
2–6	1.3971	1.4119	1.4522	1.4306	1.3856	1.4127
6–7	1.4442	1.5001	1.4323	1.4726	1.4422	1.4844
11–6	1.4222	1.3829	1.3944	1.4096	1.4282	1.3824
7–12	1.2639	1.2606	1.2568	1.2310	1.2481	1.2524
α (7, 6, 2, 1)	0	0	90	78.8	180	180
β (6, 2, 1, 5)	180	180	180	161.3	180	180

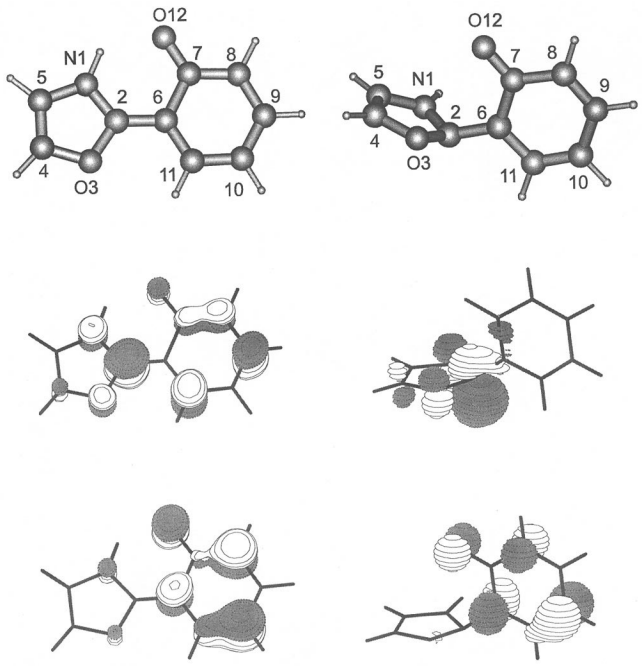

Fig. 13. Equilibrium structure NH-*cis* and structure of the NH-90 minimum on the excited-state surface, together with the corresponding frontier orbitals (LUMO upper, HOMO lower), for HPO. Similar results have been determined for HPT.

one with nonplanar oxazole subsystems (see Fig. 13, r.h.s.). This structural bending of the entire molecule is also borne out by the α and β dihedral angles in Tables 8 and 9.

This behaviour can be qualitatively understood in terms of the electronic structure of the ground and excited states of NH-90 (Scheme 2): the lower energy structure (S_0) of NH-90 corresponds to the hole-pair-type state [44,45] with reduced electron density in the positively charged oxazole or thiazole ring, with a substantial ground state dipole moment of the NH-90 form (Tables 6 and 7) and with an even number of electrons on both rings. The heteroaromatic ring therefore tends to be planar (Tables 8 and 9). The S_1 state, on the other hand, corresponds to the dot-dot species [44,45] with one electron localised in the five-membered and one in the six-membered ring, and with correspondingly increased electron density in the five-membered ring, connected with a reduced dipole moment. Consistent with previous findings on charged pyridinium systems [46], the increased electron density in the five-membered ring can lead to a rehybridisation resulting in a pyramidalised five-membered ring subsystem for the optimised S_1-NH-90 form as shown in Fig. 13and borne out by the dihedral angles in Tables 8 and 9 deviating from 180 and 90°.

The central bond length for HPO and HPT, also contained in Tables 8 and 9, shows a strong increase for the NH-90 structure in both ground and excited states. This is consistent with the valence bond resonance structures, which place a large weight of double-bond character on this bond. In the NH-90 form, this valence bond structure is not available, and the double-bond character is lost leading to the bond lengthening. A summary of the ground and excited state characteristics of the various NH-species is given in Tables 6 and 7. The S_1-state of the NH-*cis* forms of boths compounds is of π-π^* nature as well as the NH-*trans* form of HPT. But the S_1-state of the NH-*trans* form of HPO is calculated to be of n-π^* nature (Table 6).

Table 10
Properties of the optimised T_1 state for the NH-type conformers of HPO and HPT as calculated by HF/3–21G*

State characteristic	HPO		HPT	
	NH-*cis*	NH-*trans*	NH-*cis*	NH-*trans*
Point group	C_S	C_S	C_S	C_S
Energy gap of $T_1 \rightarrow S_0$, eV	1.98	1.57	1.81	1.73
Energy gap of $S_1 - T_1$[a], eV	2.14	2.66	2.00	2.10
State nature	π-π^*	π-π^*	π-π^*	π-π^*

[a] Energy gap between the equilibrium S_1 and T_1 states.

The biradicaloid dot-dot electronic structure of the NH-90 forms of HPO and HPT in the S_1-state is confirmed by the small energy gap between the S_1- and T_1-states (Tables 6 and 7and Fig. 12). Both states possess the same optimised geometry and correspond to the same dot-dot electronic configuration. Both S_1 and T_1 states possess a small dipole moment, and therefore the dipole moment change for the S_1 (or T_1) $\rightarrow S_0$-transition is very large and corresponds to the transfer of nearly a full electron. This is directly visualised by the shape of the HOMO and LUMO orbitals which are localised on the different fragments in the NH-90 form (Fig. 13).

Due to the relatively small energy gap for $S_1 \rightarrow S_0$ in the NH-90 structure (Table 10), calculated by HF/3–21G* (1.8–21 eV), the nonradiative transition from the minimum in S_1 to the ground state is likely to be important; consequently, this structure can be expected to lead to the quenching of the keto fluorescence. A further possible source of fluorescence quenching is given by the near-degeneracy of the S_1 and T_1 states of the NH-90 species (see Fig. 12).

3.4.4. Triplet state of NH-type conformers

The triplet NH-*cis* and NH-*trans* conformers are stable species (energy minima). The singlet-triplet energy difference is strongly angle-dependent. It is sizeable for planar geometries and very small for perpendicular ones (see Tables 6 and 7and Fig. 12). The near-degeneracy with S_1 for 90° is due to the biradicaloid nature of these two states (dot-dot nature) as outlined above and is connected with localisation of the molecular orbitals for this geometry.

4. Conclusion

The absorption and emission properties of HPO and HPT resemble in many respects those of the benzo analogues HPBO and HPBT. These compounds exhibit dual fluorescence in polar and protic solvents due to several ground

state tautomers. In the first excited singlet state, the quantum chemical calculations suggest the existence of two deactivation channels of the proton transfer tautomers at 90° twist. At this conformation, the S_1–S_0 energy gap is reduced, and the T_1 and S_1 states are near-degenerate. We recently proposed a similar mechanism for 2-(2′-hydroxyphenyl)pyridine [47].

The different nature of the heteroatom does affect some of the properties of the azoles. The nitrogen is less basic for the oxazole compounds than for the thiazoles. In the ground state, the *trans* isomer is more stabilised for the oxazole HPO than for HPT. The different electronic distribution is altered upon benzo substitution. The benzo analogues HPBO and HPBT are stronger emitters and a comparison of their p*K* values also shows that they are less basic than HPO and HPT, respectively.

Acknowledgements

We thank Dr. B. Crystall, Imperial College, London for access to the laser system for fluorescence lifetime measurements. This work has been supported by the Bundesministerium für Forschung und Technologie Project 05 414 SKT FAB9. The support of the Volkswagenstiftung and the German Academic Exchange program DAAD is gratefully acknowledged. We thank the University of Central Lancashire for a research studentship (DLG), EPSRC for access to the Daresbury Laboratory and BESSY (within EU programme CHGE-CT93-0027) for beamtime and travel support.

References

[1] S.J. Formosinho, L.G. Arnaut, J. Photochem. Photobiol. A: Chem. 75 (1993) 1, 21.
[2] S.M. Ormson, R.G. Brown, Progr. React. Kinet. 19 (1994) 45.
[3] D. LeGourriérec, S.M. Ormson, R.G. Brown, Progr. React. Kinet. 19 (1994) 211.
[4] R. Passerini, J. Chem. Soc. (1954) 2257.
[5] R. Passerini, A. Cerniani, R. Passerini, J. Chem. Soc. (1954) 2261
[6] D. Cohen, S. Flavian, J. Chem. Soc. B (1967) 317, 321
[7] C.A.S. Potter, R.G. Brown, F. Vollmer, W. Rettig, J. Chem. Soc. Faraday Trans. 90 (1994) 59.
[8] T. Höfer, P. Kruck, T. Elsaesser, W. Kaiser, J. Phys. Chem. 99 (1995) 4380.
[9] W. Frey, F. Laermer, T. Elsaesser, J. Chem. Phys. 95 (1991) 10391.
[10] M. Krishnamurthy, S.K. Dogra, J. Photochem. 32 (1986) 235.
[11] B. Nickel, K.H. Grellmann, J.S. Stephan, P.J. Walla, Ber. Bunsenges. Phys. Chem. 102 (1998) 436.
[12] G. Yang, Z.A. Dreger, Y. Li, H.G. Drickamer, J. Phys. Chem. A 101 (1997) 7948.
[13] D.L. Williams, A. Heller, J. Phys. Chem. 74 (1970) 4473.
[14] E.L. Roberts, J. Dey, I.M. Warner, J. Phys. Chem. 100 (1996) 19681.
[15] K. Das, N. Sarkar, A.K. Ghosh, D. Majumdar, D.N. Nath, K. Bhattacharyya, J. Phys. Chem. 98 (1994) 9126.
[16] J. Catalán, F. Fabero, M.S. Guijarro, R.M. Claramunt, M.D. Santa Maria, M. de la Conception Foces-Foces, F.H. Cano, J. Elguero, R. Sastre, J. Am. Chem. Soc. 112 (1990) 747.
[17] M. Wiechmann, H. Port, J. Lumin. 48/49 (1991) 217.
[18] M. Pfeiffer, K. Lenz, A. Lau, T. Elsaesser, J. Raman Spectrosc. 26 (1995) 607.
[19] P.-T. Chou, W.C. Cooper, J.H. Clements, S.L. Studer, C.P. Chang, Chem. Phys. Lett. 216 (1993) 300.
[20] M. Itoh, Y. Fujiwara, J. Am. Chem. Soc. 107 (1985) 1561.
[21] A.R. Katritzky, Physical Methods in Heterocyclic Chemistry, vol. 3, Academic Press, New York, 1971
[22] A.R. Katritzky, Handbook of Heterocyclic Chemistry, Pergamon Press, Oxford, 1985.
[23] A. Douhal, F. Lahmani, A. Zehnacker-Rentien, F. Amat-Guerri, J. Phys. Chem. 98 (1994) 12198.
[24] V. Guallar, M. Moreno, J.M. Lluch, F. Amat-Guerri, A. Douhal, J. Phys. Chem. 100 (1996) 19789.
[25] E.V. Brown, J. Org. Chem. 42 (1977) 3208.
[26] W.E. Cass, J. Am. Chem. Soc. 64 (1942) 785.
[27] P.G.M. Bavin, Org. Synth. Coll. 5 (1973) 30.
[28] B.S. Furniss, A.J. Hannaford, P.W.G. Smith, A.R. Tatchell, Vogel's Textbook of Practical Organic Chemistry, 5th ed., Longman, New York, 1989.
[29] L. Müslin, W. Roth, H. Erlenmeyer, Helv. Chim. Acta 36 (1953) 886.
[30] S. Scheibye, B.S. Pedersen, S-O. Lawesson, Bull. Soc. Chim. Belges 87 (1978) 229.
[31] P.A. Levene, Org. Synth. Coll. 2 (1943) 88.
[32] K. Anthony, R.G. Brown, J.D. Hepworth, K.W. Hodgson, B. May, M.A. West, J. Chem. Soc. Perkin Trans. 2 (1984) 2111.
[33] K.W. Hodgson, PhD Thesis, Lancashire Polytechnic, Preston, UK, 1986.
[34] W.H. Melhuish, J. Phys. Chem. 65 (1961) 229.
[35] R. Sparrow, R.G. Brown, E.H. Evans, D. Shaw, J. Chem. Soc. Faraday Trans. II 82 (1986) 2249.
[36] M. Vogel, W. Rettig, Ber. Bunsenges. Phys. Chem. 91 (1987) 1241.
[37] D.V. O'Connor, D. Phillips, Time-correlated single photon counting, Academic Press, London, 1984.
[38] A. Albert, E.P. Serjeant, The Determination of Ionisation Constants, Chapman & Hall, London, 1971.
[39] J. Keck, H.E.A. Kramer, H. Port, T. Hirsch, P. Fischer, G. Rytz, J. Phys. Chem. 100 (1996) 14468.
[40] F. Vollmer, W. Rettig, J. Photochem. Photobiol. 95 (1996) 143.
[41] A. Mordzinski, A. Grabowska, Chem. Phys. Lett. 90 (1982) 122.
[42] A. Mordzinski, K.H. Grellmann, J. Phys. Chem. 90 (1986) 5503.
[43] M.J. Frisch, G.W. Trucks, H.B. Schlegel, P.M.W. Gill, B.G. Johnson, M.A. Robb, J.R. Cheeseman, T. Keith, G.A. Petersson, J.A. Montgomery, K. Raghavachari, M.A. Al-Laham, V.G. Zakrzewski, J.V. Ortiz, J.B. Foresman, C.Y. Peng, P.Y. Ayala, W. Chen, M.W. Wong, J.L. Andres, E.S. Replogle, R. Gomperts, R.L. Martin, D.J. Fox, J.S. Binkley, D.J. Defrees, J. Baker, J.P. Stewart, M. Head-Gordon, C. Gonzalez, J.A. Pople, GAUSSIAN 94, Revisions B.2 and E.2, Gaussian, Inc., Pittsburgh, PA, 1995.
[44] J. Michl, V. Bonacic-Koutecký, Electronic Aspects of Organic Photochemistry, Wiley, New York, 1990.
[45] W. Rettig, Topics in Current Chemistry, in: J. Mattay (Ed.), Electron Transfer I, Springer, Berlin, vol. 169, 1994, p. 253
[46] V.A. Kharlanov, W. Rettig, M.I. Knyazhansky, N. Makarova, J. Photochem. Photobiol. A: Chem. 103 (1997) 45.
[47] D. LeGourriérec, V.A. Kharlanov, R.G. Brown, W. Rettig, J. Photochem. Photobiol. A: Chem. 117 (1998) 209.